Mechanical and Film Properties of Thermally Curable Polysiloxane

Ruby Chakraborty, Mark D. Soucek

Department of Polymer Engineering, The University of Akron, Akron, Ohio 44311-0301

Received 7 July 2008; accepted 9 November 2008
DOI 10.1002/app.29820
Published online 28 August 2009 in Wiley InterScience (www.interscience.wiley.com).

ABSTRACT: Telechelic glycidyl epoxide siloxanes substituted with either methyl, cyclopentyl, or cyclohexyl groups were cured thermally with corresponding telechelic aliphatic amine. Also, the three glycidyl epoxide functionalized siloxanes were homopolymerized via a photoinitiated cationic mechanism. Both the UV and thermal curing were performed by formulating with reactive diluents. The mechanical properties, viscoelastic behavior, and coatings properties of the thermally cured siloxanes were studied. In addition, the X-ray measurements were performed. The rate of polymerization increased with the increasing size of substituent on the siloxane backbone. The hardness, adhesion, and solvent resistance increased as the bulk of the substituent increased in the siloxane backbone. The release properties for adhesion and readhesion increased with increase in steric bulk of the backbone substituents. Crosslink density reduced and oxygen permeability increased with increase in siloxane substituent size. There was also an increase in the advancing and the receding contact angles with the increase in substituent size. The inverse dependency of substituent size and free volume was observed in the *d*-spacing of the X-ray data.
 J Appl Polym Sci 115: 358–369, 2010

Key words: telechelic; viscoelastic properties; fracture toughness; X-ray

INTRODUCTION

Polymers containing silicon are known to offer outstanding electrical[1] and weather-resistant[2] properties. The incorporation of silicon into polymeric compositions conventionally involves the use of siloxanes, hence the polymers are composed of highly stable Si—O—Si bonds.[3–5] It has been reported in the literature that higher adhesive strength was obtained with lower molecular weight epoxide resin when siloxanes are incorporated in the backbone.[6] Silicone containing epoxide derivatives are also well-known,[7] but not as widely used as BPA epoxide resin, mainly due to economic reasons. Silicone epoxy derivatives are mainly used as a silane coupling agent and for exfoliation of clay nanocomposites.[8–10]

Epoxide siloxane can be synthesized from double bond containing epoxide and silane by hydrosilation.[11] Epoxide siloxane offers the benefits of both silicone resin and epoxide resin. The siloxane bond is stable in response to heat and ultraviolet light, and epoxide resins have high adhesive strength. Synthesis and cationic polymerization of epoxide siloxane were studied by Crivello et al.[12,13] The synthesized monomers consisting of epoxycyclohexyl groups exhibited excellent reactivity in cationic ring opening polymerization. The properties of the crosslinked resins depend on the length of the siloxane backbone separating the pendant epoxide groups. Silicones are also used for toughening of epoxides. The phase separation of the siloxane component from the epoxide matrix results in a rubber toughening mechanism that effectively retards the fracture, thus improving the fracture toughness.[14–16] However, the phase incompatibility of siloxanes and BPA-epoxide leads to problems, when compounding.[17]

One of the desirable characteristics of epoxide siloxane monomer is the high reactivity. The ideal monomer can be cured with minimum catalyst concentration, and as a result the matrix will have good color stability.[18] It was reported that epoxide-substituted siloxanes can be easily polymerized by either photo-induced polymerization or thermally induced polymerization.[11] Mechanical and thermal properties of polydimethylsiloxane epoxides were investigated extensively in literature.[19–21] The mechanical properties of the resin can be directly related to the length of the polydimethylsiloxane.[18] As the length of siloxane increases, the mechanical properties of the polymer decreases.[22–25]

Epoxide functional resins are used predominately in UV-curing compositions, based on cationic homopolymerization polymerization. An important factor which retarded the development of cationic polymerization in comparison with free radical polymerization of unsaturated resins is the slower cure rates

Correspondence to: M. D. Soucek (msoucek@uakron.edu).

and dependence on relative humidity.[26,27] The slower rate of cationic polymerization is due to dominance of termination and chain transfer process at room temperature.[28] This tendency is avoided by utilizing cationic initiators with highly non-nucleophilic anions, such as PF_6^-, AsF_6^-, and SbF_6^-.[29]

Because of cost issues of amine telechelic and epoxide telechelic siloxanes, almost no applications use these together. Amine-functionalized siloxanes are used for curing conventional epoxy resins.[30] Miscibility of these functionalized siloxanes with the epoxy resins, enhances compatibility, ensures homogeneous particle distribution, and thus leads to effective toughening.[31] Interpenetrating networks having better electrical, thermal, and mechanical properties can be obtained from siloxane hybrids.[32] The interpenetrating networks are most commonly synthesized by curing alkoxy silanes with hybrid resins i.e., siloxane epoxide–conventional epoxide resin, polyol–epoxide resins, etc.[33]

The properties of films obtained by thermal curing of glycidyl epoxide functional polysiloxane and alkyl amino polysiloxane are reported in this study. A set of three glycidyl epoxide-terminated polysiloxanes were prepared with methyl, cyclopentyl, and cyclohexyl substituents, and photopolymerized with an epoxide reactive diluent using a cationic photoinitiator. The telechelic siloxane epoxides were also thermally reacted with amine-terminated methyl, cyclopentyl, and cyclohexyl substituted siloxanes. The viscoelastic and mechanical properties were evaluated using dynamic mechanical thermal analysis, stress strain measurements, and fracture toughness. Coating properties, adhesion testings, release properties, were performed. Oxygen permeability, contact angle, X-ray diffraction, chemical resistance, and impact resistance were also studied. The properties of the thermally cured systems were compared with the UV-cured glycidyl epoxide functional siloxanes.

EXPERIMENTAL

Materials and reagents

Substituted siloxanes were synthesized and functionalized with glycidyl epoxide and amine group prior to this experiment and reported previously.[34,35] The mentioned functional siloxanes were prepared from substituted dichlorosilane as starting material. Hydrolysis, ring opening polymerization with tetramethyldisiloxane, and hydrosilation of the dichlorosilane afforded the products. The glycidyl epoxide functionality was introduced by hydrosilation reaction of hydride terminated siloxane with allylglycidyl ether. For amine-terminated siloxane, *t*-butoxycarbonyl (BOC) protected allylamine was used as a hydrosilation agent, the BOC group was removed using trifluroacetic acid. Heloxy Modifier 48 and Epicure 9551 were obtained from Hexion Speciality Chemical (Columbus, OH). Acetic Acid was obtained from EMD chemicals (Gibbstown, NJ). Irgacure 250 was obtained from Ciba Speciality Chemicals (Basel, Switzerland). Aluminum panels (type A, alloy) (3 × 6 in) panels were obtained from Q-panel Lab Products (Cleveland, OH). The structures of the synthesized siloxanes, Heloxy Modifier 48, and Epicure 9551 are shown in Figure 1.

Instrumentation

Tensile and release tests were performed on an Instron 5567 (Instron Corp., Grove City, PA). The viscoelastic properties were measured on a dynamic mechanical thermal analyzer (DMTA V, Rheomtrics Scientific, Piscataway, NJ). Oxygen permeability were measured using Model 8001 Oxygen Permeation Analyzer (Illinois Instruments, Jonesburg, IL). Contact angle measurement was performed using the apparatus Rame-Hart Goniometer, model 100-00. Wide-angle X-ray diffraction (WAXD) patterns of cured specimens were generated using Bruker AXS D8 Discover X-ray diffractometer. Photo-DSC measurements were performed on a Thermal Analysis Q1000 equipped with a photo-calorimetric accessory. A Fusion UV-curing chamber (F300SQ Series) having a mercury arc bulb (150 mW cm^{-2}, UVB, 257 nm).

Coating formulation and film preparation

Aluminum and glass panels were used as substrates for film preparation. The substrates were cleaned with distilled water and acetone and dried. The thermally curable coating formulations were made by taking the synthesized glycidyl epoxide functional polysiloxane and HELOXY Modifier 48 in a glass vial and adding 0.1 wt % acetic acid, then mixing thoroughly for 20–30 min at room temperature. Then, the amine functionalized polysiloxane and Epicure 9551 was added to the glass vial and mixed again for about 15 min. The amount of the four components used are shown in Table I. The films, to be cured thermally, were cast on the substrates with a thickness of 200 μm (8 miL) by a drawdown bar. The films were cured at 120°C for 6 h and stored in a dust-free cabinet for testing purposes. In the case of UV-curable formulations, my mixing glycidyl epoxide functional siloxane, Heloxy Modifier 48, and the photoinitiator. The uniform mixtures were then cast on the substrates with a thickness of 200 μm (8 miL) by a drawdown bar, and cured using a UV-chamber. A Fusion UV-curing chamber (F300SQ Series) with a belt speed of 55 ft min^{-1} was used to cure the polysiloxanes with a UV-source (mercury arc bulb, 150 mW cm^{-2}).

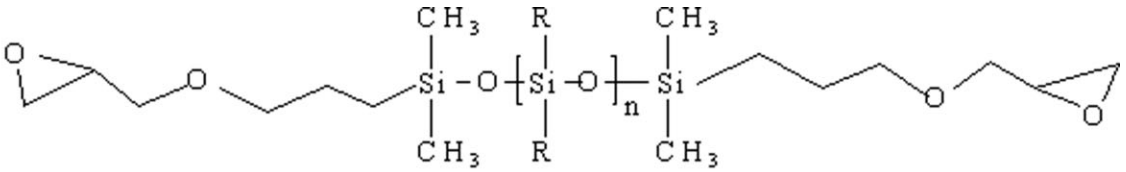

Glycidyl epoxide functional polysiloxane

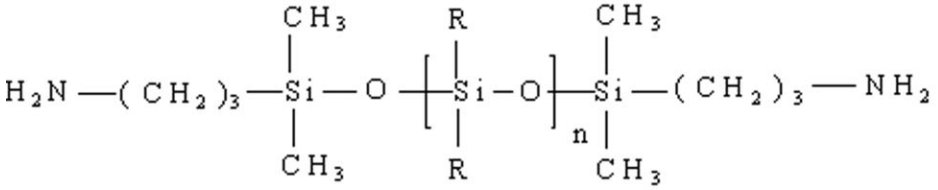

Amine functional polysiloxane

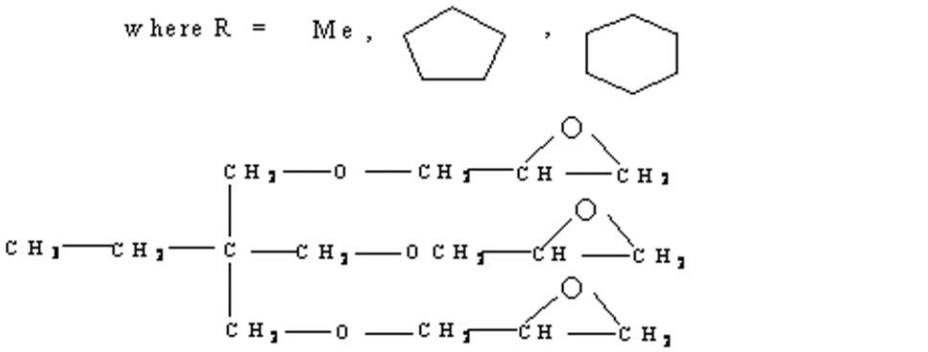

HELOXY Modifier 48 (Trimethylol propane triglycidyl ether)

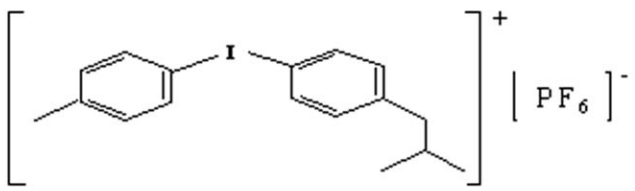

Irgacure 250

Figure 1 Structure of functionalized siloxanes, reactive diluents and photoinitiators.

TABLE I
Components of Thermally Curable Film Formation

	Glycidyl epoxide polysiloxane	Heloxy modifier 48	Amino polysiloxane	Epicure 9551
MS_Ep_NH	2.5 g, 0.0123 mol[a]	2.6 g, 0.018 mol[a]	10.32 g, 0.02 mol[b]	1.2 g, 0.01 mol[b]
PS_Ep_NH	10 g, 0.0126 mol[a]	2.6 g, 0.018 mol[a]	8 g, 0.02 mol[b]	1.2 g, 0.01 mol[b]
HS_Ep_NH	10 g, 0.0122 mol[a]	2.6 g, 0.018 mol[a]	8 g, 0.02 mol[b]	1.2 g, 0.01 mol[b]

[a] represents mol of epoxide group.
[b] represents mol of amine group.

The UV-cured homopolymerized system were abbreviated as MS_Ep (polydimethylsiloxane epoxide), PS_Ep (polydicyclopentylsiloxane epoxide), and HS_Ep (polydicyclohexyl siloxane epoxide). The thermally cured systems are abbreviated as MS_Ep_NH (polydimethylsiloxane epoxide and polydimethylsiloxane amine), PS_Ep_NH (polydicyclopentylsiloxane epoxide and polydicyclopentylsiloxane amine), and HS_Ep_NH (polydicyclohexylsiloxane epoxide and polydicyclohexylsiloxane amine). The sillicone epoxide functional and sillicone amine formulations were prepared as given in Table II.

Cured film characterization

Coating properties

After thermal curing, the general coating properties of the glycidyl epoxide functional polysiloxane/aliphatic amine polysiloxane were evaluated. The pencil hardness (ASTM D3363-74), reverse impact resistance (ASTM D 2794-84), crosshatch adhesion (ASTM D3359-87), pull off adhesion (ASTM D 4541-02), tensile properties (ASTM D 2370-92) were measured according to the ASTM standards.

Dynamic mechanical thermal analysis (DMTA)

The viscoelastic properties of the siloxane films were investigated with a dynamic mechanical thermal analyzer in a compression mode at the frequency of 1 Hz and a heating rate of 2°C/ min over a range of −160 to 150°C. The testing conditions and methodology were performed according to ASTM D 4065-95. The samples were cut into 4-mm squares with an average thickness of 0.75 mm. A minimum preload force of 200 mN was applied by the instrument. For each formulation, four replicates were tested. The crosslink density (υ_e) of the films was determined through the elastic modulus in the rubbery plateau region. The relationship between rubbery plateau modulus and crosslink density is[36]:

$$\upsilon_e = \frac{E'_{\min}}{3RT} \tag{1}$$

where υ_e is the crosslink density of elastically effective network chains, $E'_{\min}$ is the minimum value of the storage modulus (Pa) above the glass transition temperature (T_g), R is the gas constant (J/K mol) and T is the absolute temperature ($T >> T_g$) in Kelvin. At the temperature much below T_g, loss modulus (E'') is very low, therefore, modulus (E) is approximately equal to storage modulus (E'). The T_g of the specimens was considered to be the peak point of the loss modulus (E'') signal. Determination of υ_e can be performed by defining it in terms of moles of network chains per cm^3 sample, consistent with other mathematical approaches such as Graessley's.[37]

Tensile properties and fracture toughness

Tensile measurements were made on rectangular specimens 15-mm wide, 0.09 to 0.14-mm thick and with gauge length of 60 mm. A crosshead speed of 2.0 mm/min was applied to determine the tensile strength, elongation at break and tensile modulus. For each film, five samples were tested, and the average is reported. Plane-stress fracture toughness (K_{IC}) measurements were conducted on rectangular specimens with single edge notch geometry. The dimensions of the films were 60 × 15 × 0.09–0.14 mm^3 (length × width × thickness). Each film was cut with a razor blade to create a notch at approximately half the length of the specimen. The notch length was approximately 10% of the sample width. The fracture toughness equipment is mounted on a microscope stage and equipped with a 25 lbf load cell and a variable speed motor. Crosshead speed of 5 mm/min is used to deform the specimen in tensile mode. The computer digitally records the variation of load versus displacement. The crack tip region was on the computer screen at the magnification of 10× and the onset of propagation was marked on load-displacement curve. Six samples were tested for each film. The mean value was reported. The plane stress fracture toughness (K_{IC}) is given by the equation[38]:

$$K_{IC} = \left[3.94\left(\frac{2w}{\pi a}\right)\tan\left(\frac{\pi a}{2w}\right)\right]^{1/2}\frac{F}{(w-a)b}\sqrt{a} \tag{2}$$

where w is the sample width in cm, a is the notch length in cm, b is the thickness in cm, F is the force on sample at which crack propagation begins measured in Newtons.

The energy release rate per unit of crack area at fracture (G_{IC}) was calculated with the following equation:

$$G_{IC} = \frac{K_{IC}^2}{E} \tag{3}$$

where E is the tensile modulus. The G_{IC} values were calculated with average values of K_{IC} and E.

Oxygen permeability

Oxygen permeation analysis is performed to provide accurate measurements of oxygen permeation rates (OTR) through flat films and packages. The cross sectional view of the oxygen permeability apparatus is given in Figure 2. Flat film samples are clamped

TABLE II
Components of UV-Curable Film Formation

	Glycidyl epoxide polysiloxane	Heloxy modifier 48	Photoinitiator (Irgacure 250)
MS_Ep	2.5 g, 0.0123 mol[a]	2.6 g, 0.018 mol[a]	0.26 g[b]
PS_Ep	10 g, 0.0126 mol[a]	2.6 g, 0.018 mol[a]	0.63 g[b]
HS_Ep	10 g, 0.0122 mol[a]	2.6 g, 0.018 mol[a]	0.63 g[b]

[a] represents mol of epoxide group.
[b] represents 5 wt % photoinitiator.

in a diffusion chamber and pure O_2 is then introduced into the upper half of the chamber while an oxygen-free carrier gas flows through the lower half.

Molecules of oxygen diffusing through the film into the lower chamber are conveyed to the sensor by the carrier gas. This allows a direct measurement of the oxygen without using complex extrapolations. The OTR rate of the test film is displayed either as cc/100 in^2/day or cc/m^2 /day.

Contact angle measurement

Contact angle measurements were performed with a Rame-Hart contact angle goniometer, model 100-00 using deionized water. Images of advancing and receding angles were taken using image-capturing equipment (Dazzle DVC, Dazzle media). Contact angle on both sides of the droplet were measured using Scion Image at ambient conditions (1 atm, $\sim$ 25°C). Five measurements were taken for each sample and an average value of all the contact angles is reported.

Release testing by pull of adhesion

To measure adhesion of Al plates to substrate film, the following procedure has been optimized.[39,40] The formulations were casted on Al plates and cured thermally at 120°C, and then the Scotch Tape 249 was applied on the coated substrate. A 1-lb load was rolled over it five times to ensure adhesion. The release force of the tape from the cured silicone layer was measured at 180° peeling angle using tensile tester. After the tape was removed from the silicone layer, subsequent adhesion was determined by reapplying the tape to a clean steel panel, rolling five times with 1-lb roller, and again measuring the force required to remove the tape at an angle of 180°. The release energy (G) is given by:

$$G = \frac{F}{b}(1 - \cos\ \theta) \tag{4}$$

where F is steady-state peel load, b is the width of scotch tape and θ is the peel angle.[41] A minimum of five trials was conducted on each sample and the mean was reported. For this experiment, the peel angle is 180°.

Wide angle X-Ray diffraction (WAXD)

WAXD of thermally cured siloxane films were taken with Bruker X-Ray diffractometer at wavelength (λ) of 0.154 nm with tube voltage of 40 kV and tube current of 40 mA. A scanning range of 2θ from 5° to 30° with scanning interval of 0.05° were used.

Photo-differential scanning calorimetry (PDSC)

Samples were analyzed on a Thermal Analysis Q DSC 1000 equipped with a photo-calorimetric accessory. The photocalorimetric accessory included transfer optic cables to produce UV light of varying intensity and a monochromatic filter to produce light at a specific wavelength. The initiation light source was a 100 W mercury arc lamp. The polymerization reactions were run isothermally at various temperatures to regulate the heat released during polymerization. The samples were placed in uncovered hermetic aluminum DSC pans and cured with various intensities and exposure times.

The rate of propagation (R_p) is directly proportional to the rate at which heat is released from the reaction. As a result, the area of DSC exotherm can be used in conjunction with other sample information to quantify the rate of polymerization. The rate formula used in the analysis of the photopolymerization data was[42,43]:

$$R_p = \frac{\left(\frac{Q}{S}\right)M}{n\Delta H_R m} \tag{5}$$

where (Q/S) = Heat flow per second released during the reaction in J/s, M = Molar mass of the reacting species, n = Average number of epoxide group per polymer chain, and m = mass of the sample. For the cationic polymerization of glycidyl epoxide functionalized siloxanes, light intensity was 300 mW/cm^2.

RESULTS AND DISCUSSION

The cycloaliphatic-substituted telechelic siloxane epoxides were homopolymerized via a cationic UV-

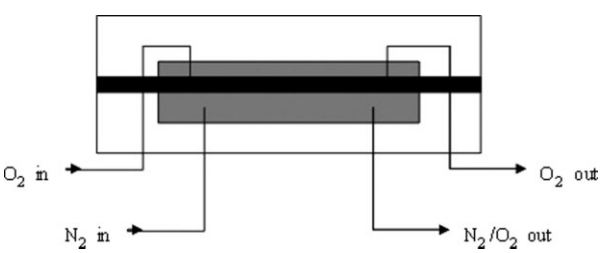

Figure 2 Cross section of sample chamber of oxygen permeability apparatus.

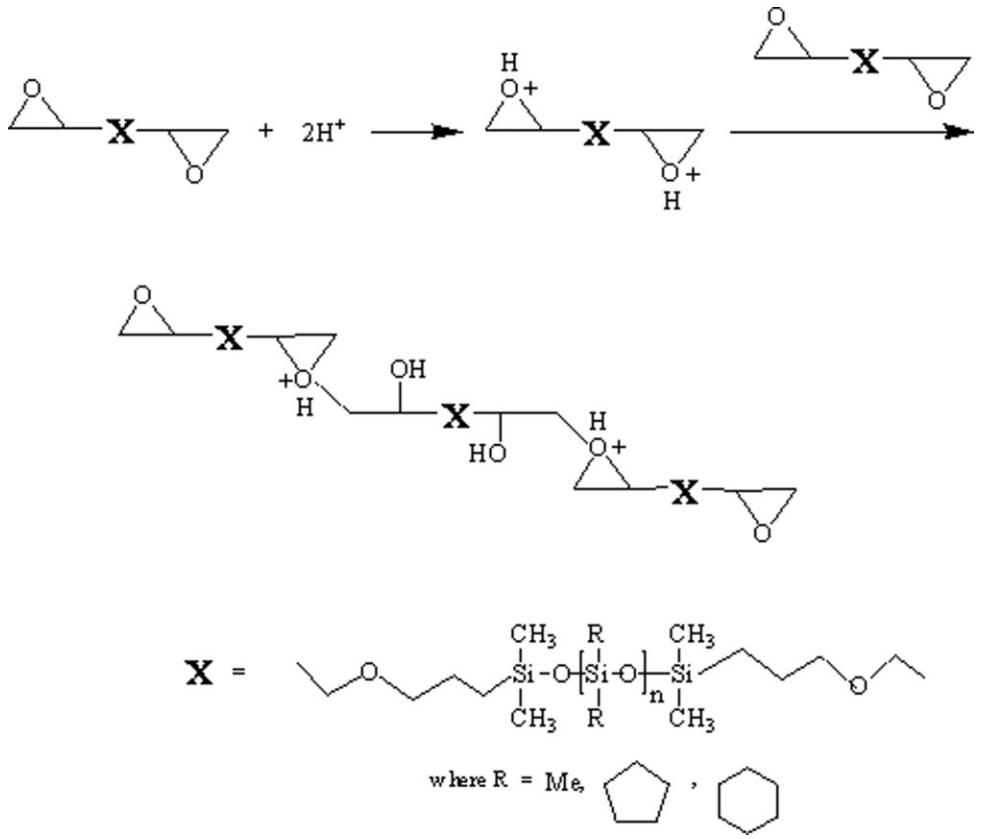

Figure 3 Schematic representation of UV-initiated homopolymerization of telechelic epoxide siloxane

curing mechanism as shown in Figure 3. The epoxides were also thermally cured with the corresponding telechelic amine-functionalized siloxanes as shown in Figure 4. The synthetic approaches for attaching the glycidyl epoxide and amine groups onto the ends of the siloxane have been recently reported.[30,31] Acetic acid was observed to accelerate the thermal cure at 120°C and consequently was

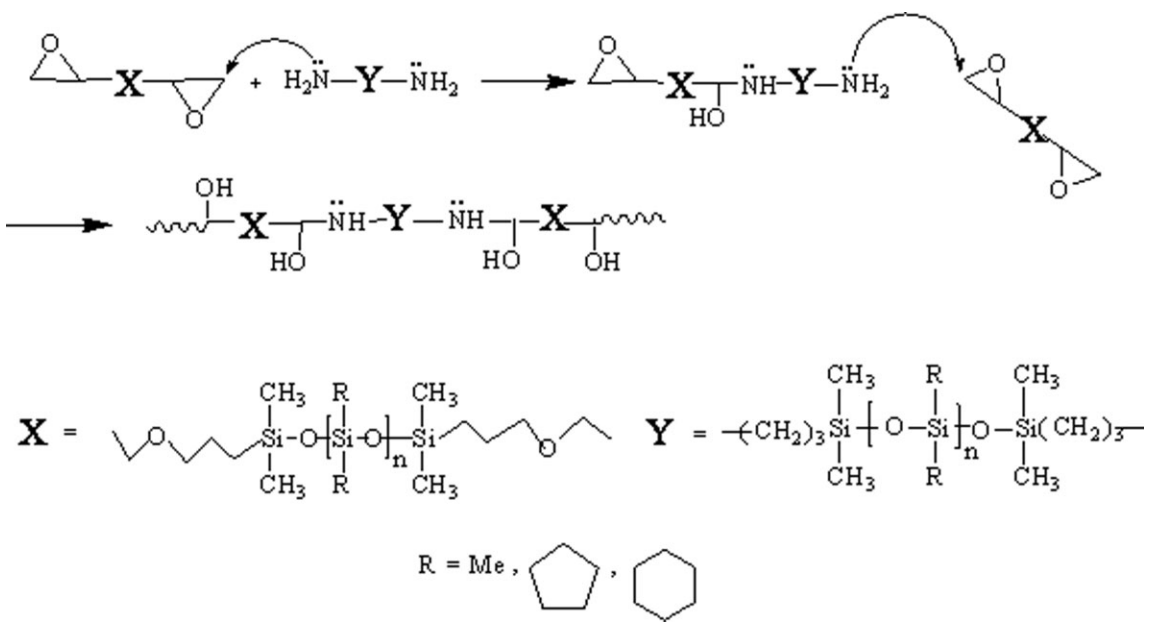

Figure 4 Schematic representation of thermal curing reaction between telechelic epoxide and amine siloxane.

chosen as a curing catalyst for this study. The addition of phosphoric acid, diethylenetriamine (DETA), diazabicyclo[2.2.2]octane (DABCO), or triethylamine (TEA) gave either very weak or almost no DSC exotherm, and thus were not effective in catalyzing the silicone–epoxide/silicone–amine reaction.

One of the target usages of the thermally curable siloxanes are for release coatings. A qualitative idea of the extent of cure was obtained by MEK double rubs of silicone-epoxide/silicone-amine were used to optimally choose the catalyst for silicone-epoxide/silicone-amine curing. The catalyst, which gave the film with largest number of MEK double rubs, was chosen. When silicone–epoxide resins were cured with the silicone–amine, very soft films were obtained. To obtain continuous films for mechanical and coating testings, HELOXY MODIFIER 48 and Epicure 9551 were added as reactive diluents in film formulations. The amount of reactive diluents was, however, minimized to ensure that it did not dominate the end properties of the siloxane films.

The thermal curing of glycidyl epoxide and amine system were observed through DSC. Each of the siloxane systems showed exothermic cure curve as shown in Figure 5. This thermogram is similar and representative of the other two systems (methyl and cyclohexyl siloxanes). The heat of reaction is given in Table III. The heat of curing reaction was determined for epoxide–amine systems with and without reactive diluents. The heat of reaction for the combination of the siloxanes and reactive diluents are much higher than cured siloxane systems alone. Not surprisingly, the reactive diluents being small molecules aided in the completeness of the cure. Consequently, films for characterizations were formed by curing siloxane with reactive diluents to obtain representable mechanical properties.

The rate of homopolymerization of the epoxidized siloxanes was obtained using photo-DSC. The overall heat of reaction, including initiation, propagation, and termination can be measured as:

$$E_R = E_P + E_I - E_T \tag{6}$$

For the validity of the above equation, production of active cationic centers must be distributed throughout the reaction.[44] The rate of propagation of a photoinitiated reaction is proportional to the height of PDSC exotherm, since most of the heat is due to the propagation. Figure 6, shows the overlay of exotherm for cationic polymerization of PDMS_Ep, PDPS_Ep, and PDHS_Ep, respectively, at 60°C for 10 s. Figure 7 depicts exotherm for cationic polymerization of PDPS_Ep at three different combinations of time and temperature. It was found that for a particular siloxane, when the exposure time was kept constant, and the temperature was increased, the rate of polymerization increases, e.g., Figure 7(a,c). It was observed (Fig. 6) for UV-cured epoxides telechelic siloxanes that as the bulk of the pendant group increased at the siloxane backbone, the rate of polymerization also increased. With increase in bulk of the pendant group, the epoxy equivalent increases, i.e., the number of epoxide group present at a given weight of siloxane polymer decreases. The free volume between each epoxide group was more, leading to an increase in mobility of superacid moiety (H^+) in the resin matrix. Thus, an increase in the efficiency of conversion. A similar effect was observed in the polymerization of multifunctional acrylates.[45]

Tensile, DMTA, and fracture toughness were performed to determine the general mechanical properties of the three thermally cured and UV-cured siloxane systems. A DMTA was used to determine the crosslink density and glass transition temperature (T_g) of the cured systems as given in Table IV and Table V. The Tan δ plots of the termally cured siloxanes are given in Figure 8. The crosslink densities were calculated from the modulus on the rubber plateau and the corresponding temperature ($T \gg T_g$) using eq. (1). The T_g was obtained as the maximum of tan δ. The same trend in T_g was observed in both DSC and DMTA. As the size of the backbone substituents increased the crosslink density decreased, thus, sterics and packing had an effect on the crosslink density. It was found that glass transition temperatures of polymers can be controlled by adding suitable pendant group through hydrosilation. As the pendant groups were varied from methyl to cyclopentyl to cyclohexyl, the T_g was observed to increase from −104 to 82°C. With increase in the bulk of pendant group rotation along Si—C bond becomes more hindered. Thus, a more rigid system results and crosslinking reactions between glycidyl epoxide telechelic siloxane and aliphatic amine telechelic siloxanes are slowed.

The plane stress fracture toughness (K_{IC}) was also found to be increasing with increase in size of the pendant group. This may be due to the fact that as the backbone pendant group of a polymer becomes bulkier, the rotational freedom of the substituents along Si—O—Si is inhibited, flexibility reduces, and toughness increases. With increase in size of the substituents in the backbone, a reduction in crosslink density is observed. Young's modulus of the thermally cured matrix increased, hence more energy is released for the crack to propagate, hence G_{IC} increases as the substituents size increased.

The overall mechanical properties of UV-curable and thermally curable siloxanes showed a mixed trend as given in Table IV and Table V, respectively. The tensile modulus of UV-cured polydimethylsiloxane and polydicyclohexylsiloxane siloxanes were higher than the corresponding

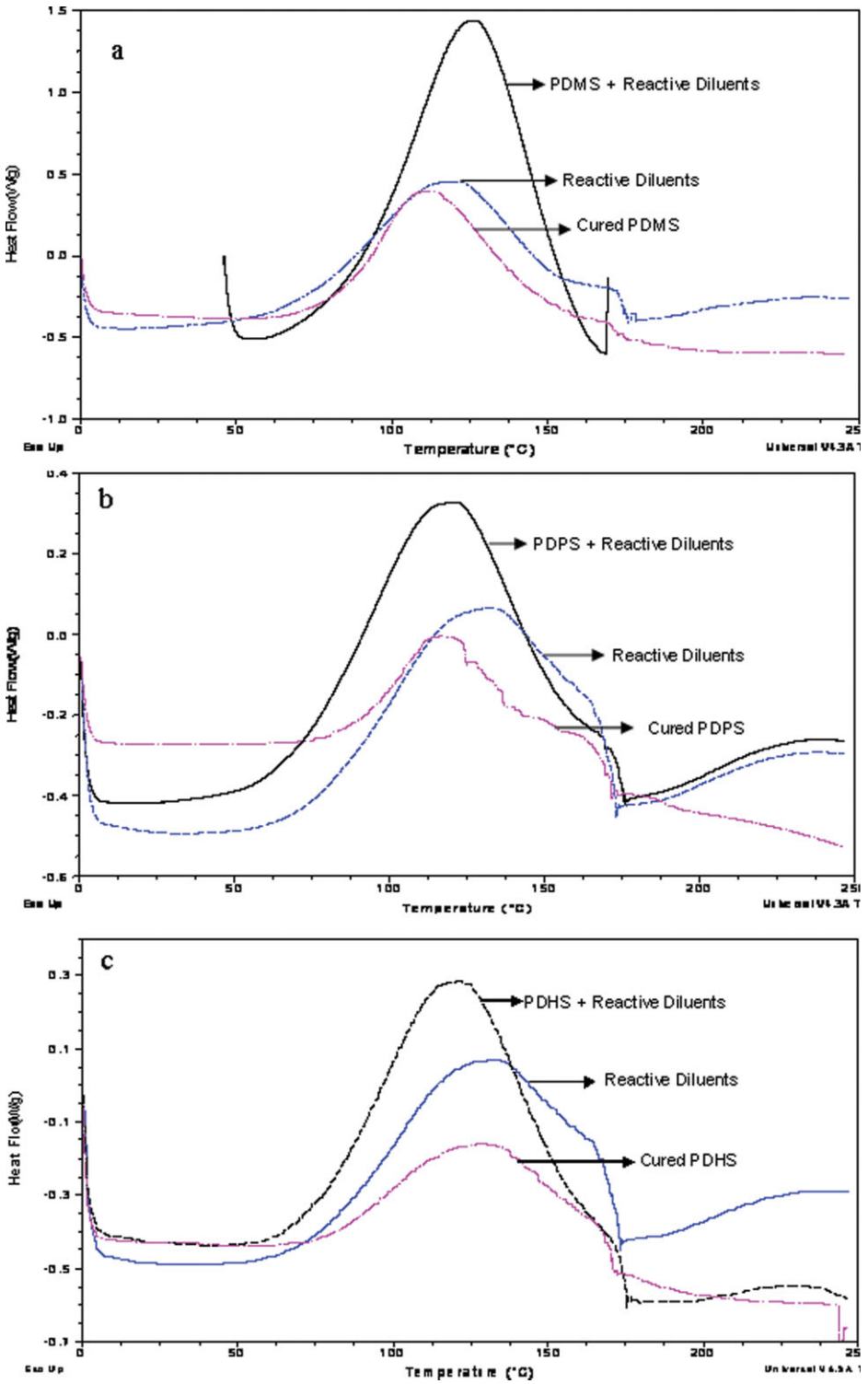

Figure 5 Curing exotherm of (a) telechelic epoxide and amine polydimethylsiloxane (PDMS), reactive diluents (Heloxy modifier 48 and Epicure 9551), and cured siloxane with reactive diluents, (b) telechelic epoxide and amine polydicyclopentylsiloxane (PDPS), reactive diluents (Heloxy modifier 48 and Epicure 9551), and cured siloxane with reactive diluents, and (c) telechelic epoxide and amine polydicyclohexylsiloxane (PDHS), reactive diluents (Heloxy modifier 48 and Epicure 9551), and cured siloxane with reactive diluents. [Color figure can be viewed in the online issue, which is available at www.interscience.wiley.com.]

thermally cured siloxanes while PDPS showed the opposite trend. The tensile strength for all the three UV-cured siloxanes were higher than the thermally cured siloxanes. The fracture toughness, elongation-to-break, and energy release rate of UV-cured siloxanes were lower than thermal cured siloxanes.

TABLE III
Heat of Curing for Polysiloxanes and Reactive Diluents

Sample name	Cured composition	Heat (J/g)
PDMS	Polydimethylsiloxane epoxide and polydimethylsiloxane amine	251.4
PDPS	Polydicyclopentylsiloxane epoxide and polydicyclopentylsiloxane amine	97.4
PDHS	Polydicyclohexylsiloxane epoxide and polydicyclohexylsiloxane amine	127.4
Reactive diluents	Heloxy 48 + Epicure 9551	208.8
PDMS + Reactive diluents	Polydimethylsiloxane epoxide Polydimethylsiloxane amine Heloxy 48 Epicure 9551	562.2
PDPS + Reactive diluents	Polydicyclopentylsiloxane epoxide Polydicyclopentylsiloxane amine Heloxy 48 Epicure 9551	277.5
PDHS + Reactive diluents	Polydicyclohexylsiloxane epoxide Polydicyclohexylsiloxane amine Heloxy 48 Epicure 9551	285.4

Though the number of moles of epoxide functionality in both UV-cured and thermally cured systems were the same, the crosslink density of UV-cured siloxanes were considerably less than the thermally cured siloxanes. This may be attributed to the fast UV-curing process, which does not allow all the reactive groups to participate in the crosslinking process. Thus, the films are cured only at the surface, and have high modulus. Crosslink densities of UV-cured siloxanes are lower than the thermal cured systems.

The tensile strength, elongation-at-break, and tensile modulus of the UV-cured and thermally cured films are given in Table IV and Table V, respectively. The tensile strength of the cyclohexyl siloxane system was highest at 5.4 MPa, more than five times higher than the methyl-substituted siloxane system. Tensile modulus of the cyclohexyl system was 2.5 times higher than the methyl substituted siloxane at 187 Pa. The elongation-to-break (%) of methyl siloxane was 9%, six times higher than the cyclohexyl siloxane system. It was observed that as the bulk of pendant group increases, the tensile modulus and strength was increased and the elongation-at-break decreased.

The general film properties for the three thermally cured systems is summarized in Table VI. Usually, the larger the organic substituents on the siloxane backbone, lower release properties are observed, thereby improving the adhesion of PSAs.[46] As the pendant group in the silicone backbone was varied from methyl to cyclopentyl to cyclohexyl, the backbone becomes more rigid. Hence, the segmental mobility reduces resulting in a denser network. Readhesion values increase significantly for all the systems. Pencil hardness of a cured film is related to

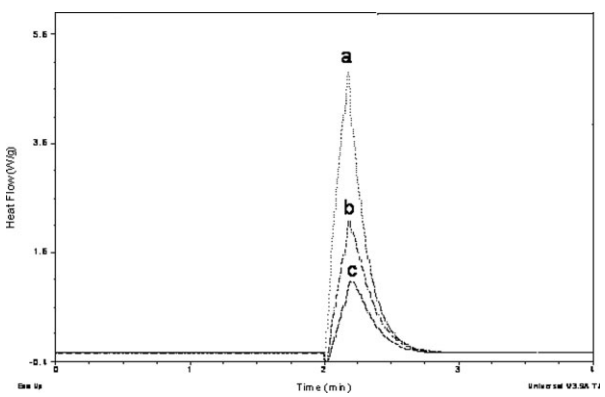

Figure 6 Exotherm for cationic photopolymerization of glycidyl epoxide functionalized (a) polydicyclohexylsiloxane (PDHS) (b) polydicyclopentylsiloxane (PDPS) and (c) polydimethylsiloxane (PDMS) at 60°C for 10 s.

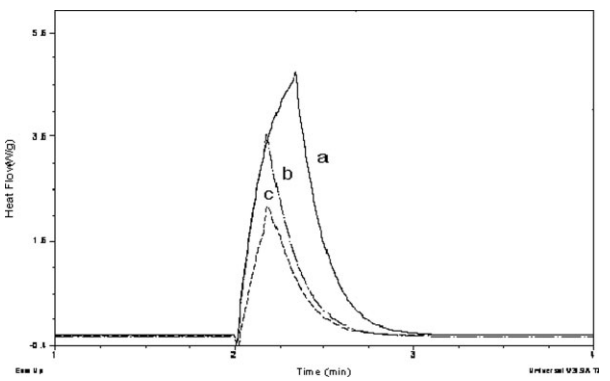

Figure 7 Exotherm for cationic photopolymerization of glycidyl epoxide functionalized polydicyclopentylsiloxane (PDPS) (a) at 60°C for 10 s, (b) at −10°C for 20 s, and (c) at −10°C for 10 s.

TABLE IV
The Mechanical Properties of UV-Cured Siloxanes

	MS_Ep	PS_Ep	HS_Ep
Tensile Modulus (Pa)	89.0 ± 5.1	143.0 ± 12.7	204.0 ± 17.4
Tensile Strength (Pa)	1.8 ± 0.5	6.2 ± 2.4	6.9 ± 1.9
Elongation-to-break (%)	0.70 ± 0.01	0.08 ± 0.01	0.05 ± 0.01
υ_e (mol/m^3)	1562	671	598
K_c (MPa m$^{1/2}$)	0.008 ± 0.002	0.050 ± 0.009	0.080 ± 0.010
G_{IC} (J m^{-2})	20.0 ± 2.6	57.0 ± 6.1	68.0 ± 7.7

the elongation-at-break, i.e., the coating is broken only when the maximum stress due to the pencil or indenter scratching exceeds the tensile strength of the coating film. Therefore, the pencil hardness shows the same trend as the tensile properties. With increase in substituent size, the pull-off adhesion is increased. This may be attributed to increase in toughness.

The falling weight impact test was performed to determine the ability of the coating to resist damage caused by rapid deformation (impact). The resistance of the coating to the penetration by the falling weight is directly proportional to strength of the coating matrices. So, in this case both for reverse and direct impact testing energy that the coating can withstand increased with increase in bulkiness of the pendant group attached to silicone backbone. Impact resistance was found to be directly proportional to the fracture toughness. A high value of fracture toughness and impact resistance in the absence of crack is the reflection of good resistance to crack initiation and crack propagation. It was found that as the bulkiness of the pendant group in the silicone backbone increased, the adhesion strength, and MEK resistance increased, and crosslink density decreased. Crosshatch adhesion values of thermally cured PDPD and PDHS was observed to be much higher than the PDMS system.

Oxygen permeability values were found to increase with increase in the bulk of the pendant

TABLE V
The Mechanical Properties of Thermally Cured Siloxanes

	MS_Ep_NH	PS_Ep_NH	HS_Ep_NH
Tensile modulus (Pa)	73.00 ± 1.68	156.00 ± 2.15	187.00 ± 2.02
Tensile strength (Pa)	0.8 ± 0.1	4.8 ± 0.4	5.4 ± 0.1
Elongation-to-break (%)	1.80 ± 0.87	0.40 ± 0.07	0.30 ± 0.04
υ_e (mol/m^3)	2935	228	115
K_c (MPa m$^{1/2}$)	0.07 ± 0.01	0.15 ± 0.05	0.26 ± 0.06
G_{IC} (J m^{-2})	67.1 ± 5.6	144.2 ± 9.2	361.5± 15.4

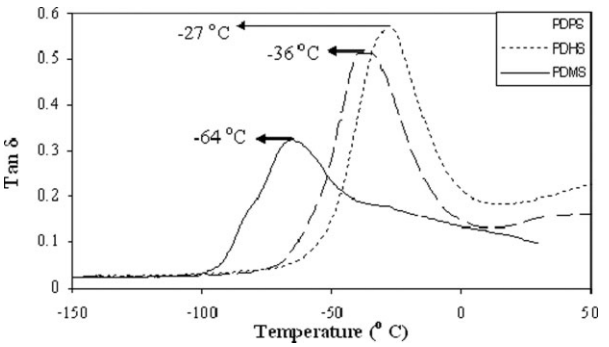

Figure 8 Tan δ plot of thermally cured polydimethylsiloxane (PDMS), polydicyclopentylsiloxane (PDPS), and polydicyclohexylsiloxane (PDHS).

group. This was due to the fact that as the steric bulk of the organic groups attached to the silicone backbone increases, the sites of crosslinking become further apart. The free volume of the cured polymer matrix increases and hence the oxygen transmission rate rises. Both the advancing and receding contact angle increase with the increase in hydrophobicity of the thermally cured siloxane layer on the silicone wafer. The methyl substituted siloxane is the least hydrophobic and cyclohexyl substituted siloxane is the most hydrophobic.

The X-ray diffraction pattern of the three thermally cured siloxanes is shown in Figure 9. The packing density of the cured siloxane specimens were studied by WAXD. All the samples exhibit a broad peak indicating amorphous nature of these samples. The *d*-spacing in the diffraction pattern, which characterize the chain to chain distance in the polymer matrix was calculated using Bragg's equation as shown here:

$$n\lambda = 2d \sin\theta \tag{7}$$

where θ is the angle of maximum intensity of the peak observed in the sample spectrum and λ is the wavelength of the X-ray radiation. As the bulkiness of the pendant group on the siloxane main chain is increasing, the peak intensity is found to decrease. There is a small shift in the peak position, as the pendant group varies from methyl ($2\theta = 17.7^\circ$, *d*-spacing value of 2.5 A°), to cyclopentyl ($2\theta = 16.6^\circ$, *d*-spacing value of 2.7 A°), to cyclohexyl ($2\theta = 15.45^\circ$, *d*-spacing value of 2.9 A°). The broadness is most likely an overlap of the unreacted oligomers and the lack of packing of the cycloaliphatic substituents. The increase in *d* spacing supports the DMTA and oxygen permeability results that, as the steric bulk of pendant group in the siloxane backbone increases the crosslink density decreases, oxygen permeability increases and polymer chain to chain distance within the polymer matrix increases.

TABLE VI
Coating Properties of Thermally cured PDMS, PDPS, and PDHS

		MS_Ep_NH	PS_Ep_NH	HS_Ep_NH
Release energy (N/m)	Adhesion	40.0 ± 7.5	120.0 ± 3.7	130.0 ± 5.0
	Readhesion	60.0 ± 6.8	160.0 ± 4.0	220.0 ± 9.1
Pencil hardness		B	2H	2H
Cross-hatch adhesion		B	4B	4B
Pull-off adhesion (N/mm^2)		0.38	0.50	0.50
MEK resistance (Double rubs)		20.0 ± 1.3	40.0 ± 2.9	45.0 ± 0.8
Impact resistance (lb/in)	Direct	>40	>40	>40
	Reverse	10.0 ± 0.5	25.0 ± 1.3°	30.0 ± 1.7
Contact angle	Advancing	90° ± 0.75°	104° ± 0.40°	115° ± 0.31°
	Receding	70° ± 2.08°	77° ± 2.52°	90° ± 4.44°
O_2 permeability (barrer)		0.02 ± 0.00	0.09 ± 0.01	0.63 ± 0.07

As previously reported,[37] an unusual relationship between free-volume, T_g, and curing exists for cycloaliphatic substituted siloxanes. It has been surmised that due to packing of the cycloaliphatic group. For both the methyl and phenyl group the packing is driven either by size or dipole-dipole effects, respectively. The cycloaliphatics bring the unique feature of a higher usage temperature (T_g), and greater free volume. This will be useful for a number of applications, i.e., membranes,[47,48] and coating applications.[49,50]

CONCLUSIONS

The glycidyl epoxide functionalized methyl, cyclopentyl, or cyclohexyl siloxanes can be homopolymerized or reacted thermally with an aminoplast hardner. A reactive diluent was needed for film formation in both the UV-curable homopolymerized siloxane epoxides and for the thermally cured siloxane epoxide-amine. The tensile strength and modulus of UV-cured homopolymerized siloxanes were found to be greater than the corresponding thermal cured siloxanes. The fracture toughness and elongation-to-break of thermal cured siloxanes were larger than the UV-cured siloxanes. It was found that overall mechanical and coatings properties of thermally cured siloxanes improved with increase in bulk of the pendant group in the backbone. The hydrophobicity increased with increase in steric bulk of the side groups as evidenced by an increase in contact angles and release forces. Also, crosslink density increased and oxygen permeability decreased with increase in the size of pendant group. The rate of cationic polymerization was observed to increase with increase in bulk of the side groups.

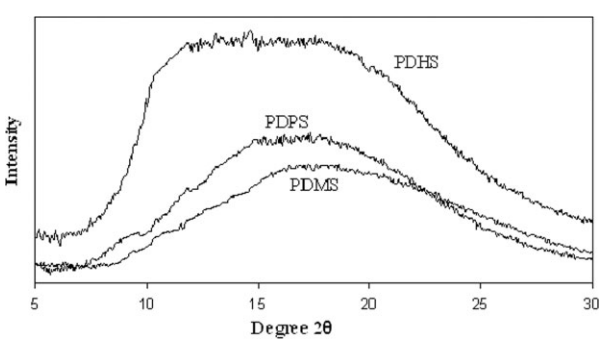

Figure 9 WAXD spectrum of thermally cured siloxanes.

References

1. Voorhoeve, R. J. H. Organohalosilanes, Precursors to Silicones; Elsevier Publishing: New York, 1967.
2. Noll, W. Chemistry and Technology of Silicones; Academic Press: New York, 1968.
3. Pekar, H. G.; Kinkelaar, E. W. U.S. Pat. 4,737,385 (1988).
4. Riffle, J. S.; Yilgor, I.; Banthia, A. K.; Wilkes, G. L.; McGrath, J. E. Org Coat Appl Polymer Sci Proc 1981, 46, 397.
5. Riffle, J. S.; Yilgor, I.; Tran, C.; Wilkes, G. L.; McGrath, J. E.; Banthia, A. K. ACS Sym Ser 1983, 221, 21.
6. Ryntz, R. A.; Gunn, V. E.; Zou, H.; Duan, Y. L.; Xiao, H. X.; Frisch, K. C. J Coat Technol 1992, 64, 83.
7. Morita, Y. J Appl Polym Sci 2005, 97, 946.
8. Plueddemann, E. P.; Fanger, G. J Am Chem Soc 1959, 81, 2632.
9. Kerr, S. R. Adhes Age 1998, 41, 27.
10. Wang, K.; Wang, L.; Wu, J.; Chen, L.; He, C. Langmuir 2005, 21, 3613.
11. Crivello, J. V.; Lee, J. L. J Polym Sci Part A: Polym Chem 1990, 28, 479.
12. Crivello, J. V.; Song, K. Y.; Ghoshal, R. Chem Mater 1932, 2001, 13.
13. Jang, M.; Crivello, J. V. J Polym Sci Part A: Polym Chem 2003, 41, 3056.
14. Fdez de, N. F.; Llano-Ponte, R.; Mondragon, I. Polymer 1996, 37, 1589.
15. Jayle, L.; Bucknall, C. B.; Partridge, I. K.; Hay, J. N.; Fernyhough, A.; Nozue, I. Polymer 1996, 37, 1897.
16. Yilgor, E.; Yilgor, I. Polymer 1998, 39, 1691.
17. Hou, S.-S.; Chung, Y.-P.; Chan, C.-K.; Kuo, P.-L. Polymer 2000, 41, 3263.
18. Morita, Y.; Tajima, S.; Suzuki, H.; Sugino, H. J Appl Polym Sci 2006, 100, 2010.
19. Dong, J.; Liu, Z.; Feng, Y.; Zheng, C. J Appl Polym Sci 2006, 100, 1547.
20. Okamoto, T.; Nakamura, S. Jpn J Appl Phys 2008, 47, 521.
21. Zhong, H.; Rubinsztajn, S. U.S. Pat. 7,013,965 (2006).
22. Rey, L.; Poisson, N.; Maazouz, A.; Sautereau, H. J Mater Sci 1999, 34, 1775.

23. Ioan, S.; Grigorescu, G.; Stanciu, A. Polymer 2001, 42, 3633.
24. Ioan, S.; Grigorescu, G.; Stanciu, A. Eur Polym Mater 2002, 38, 2295.
25. Tyagi, D.; Wilkes, G. L.; Yilgor, I.; McGrath, J. E. Polym Bull 1982, 8, 543.
26. Decker, C.; Viet, T. N. T.; Thi, H. P. Polym Int 2001, 50, 986.
27. Chen, J.; Soucek, M. D. Eur Polym Mater 2003, 39, 505.
28. Ledwith, A.; Sherrington, D. C. In Reactivity and Mechanism in Polymerization by Complex Organometallic Derivatives; Jenkins, A. D.; Ledwith, A., Eds.; Wiley Interscience: New York, 1974; pp 383–430.
29. Pappas, S. P. Radiation Curing—Science and Technology; Plenum Press: New York, 1992.
30. Srividhya, M.; Lakshmi, M. S.; Reddy, B. S. R. Macromol Chem Phys 2005, 206, 2501.
31. Bregg, R. K. Frontal Polymer Research; Nova Publishers: New York, 2005; p 37.
32. Velan, T. V. T.; Bilal, I. M. Def Sci J 2002, 52, 87.
33. Wu, S.; Sears, M. T.; Soucek, M. D. Prog Org Coat 1999, 36, 89.
34. Chakraborty, R.; Soucek, M. D. Macromol Chem Phys 2008, 209, 604.
35. Duplock, S. K.; Matisons, J. G.; Swincer, A. G.; Warren, R. F. O. J Inorg Organomet 1991, 1, 361.
36. Wicks, Z. W., Jr.; Jones, F. N.; Pappas, S. P. Organic Coating: Science & Technology, Volume II: Applications, Properties and Performance; Wiley: New York, 1994.
37. Graessley, W. W. Advances in Polymer Science, Vol. 16: The Entanglement Concept in Polymer Rheology; Springer: New York, 1974; p 179.
38. Ballard, R. L.; Sailer, R. A.; Larson, B.; Soucek, M. D. J Coat Technol 2001, 73, 107.
39. Kinloch, A. J. Adhesion and Adhesives; Chapman and Hall: London 1987.
40. Langowski, H. C.; Moosheimer, U. Vacuum Web coating of polymers: An update on European collaborative R&D. activities. Proceedings of the 42nd Annual Technical Conference, Chicago 1999; p. 387.
41. Georgiou, I.; Hadavinia, H.; Ivankovic, A.; Kinloch, A. J.; Tropsa, V.; Williams, J. G. J Adhes 2003, 79, 239.
42. Harris, K. S.; Wang, C. M.; Bowman, C. N. Macromolecules 1994, 27, 650.
43. Guymon, C. A.; Bowman, C. N. Macromolecules 1997, 30, 1594.
44. Dworak, D. P.; Soucek, M. D. Prog Org Coat 2003, 47, 448.
45. Crivello, J. V.; Lee, J. L.; Conlon, D. A. J Radiat Curing 1983, 10, 6.
46. Auner, N.; Weis, J. Organosilicon Chemistry V; Wiley-VCH GmbH: Weinheim, Germany, 2003; p 632.
47. Dworak, D. P.; Lin, H.; Freeman, B. D.; Soucek, M. D. J Appl Polym Sci 2006, 102, 2343.
48. Senthilkumar, U.; Reddy, B. S. R. J Membr Sci 2004, 232, 73.
49. Wyman, J. E. U.S. Pat. 5,096,738 (1990).
50. Ritscher, J. S.; Reedy, J. D.; Hartman, K. W. U.S. Pat. 5,359,109 (1993).